

Voltage and Frequency Support Scheme for Storage Systems in Distribution Grids

Anastasis Charalambous, Lenos Hadjidemetriou, and Elias Kyriakides
KIOS Research and Innovation Center of Excellence and Department of Electrical and
Computer Engineering, University of Cyprus
P.O. Box 20537 CY-1678
Nicosia, Cyprus
Tel.: +357/22-893450
Fax: +357/22-894555
E-Mail: {charalambous.anastasis, hadjidemetriou.lenos, elias}@ucy.ac.cy
URL: <http://www.kios.ucy.ac.cy/>

Acknowledgements

This work is supported in part by the Research Promotion Foundation (RPF, Cyprus, Project KOINA/SOLAR-ERA.NET/1215/06), by the Ministry of National Infrastructure Energy and Water (Israel) and the SOLAR-ERA.NET (European Union's Seventh Framework Programme). Further, the work is also supported in part by the European Union's Horizon 2020 research and innovation programme under grant agreement No 739551 (KIOS CoE) and from the Government of the Republic of Cyprus through the Directorate General for European Programmes, Coordination and Development.”

Keywords

Converter control, Energy storage, Fault-ride-through, Flywheel, Smart grids.

Abstract

Power electronics converters can enable grid support functionalities under abnormal grid conditions. In this paper, a voltage-frequency support strategy based on the reactance to resistance (X/R) ratio of the grid impedance is proposed for a flywheel energy storage system. Unlike conventional support schemes where voltage and frequency support is decoupled, the proposed strategy considers the coupling between voltage and frequency due to the resistive characteristics of the grid impedance in low voltage distribution grids. In addition, the proposed strategy ensures a fair compensation between voltage and frequency support by utilizing two gains that are defined according to the event type. Simulations and experimental tests are carried out using a laboratory setup to validate the proposed strategy. The capabilities of storage systems to provide such tailor-made ancillary services for supporting the distribution grid are demonstrated.

1. Introduction

The distribution grid is currently undergoing substantial challenges due to the massive integration of power electronics based renewable generation [1]. The voltage and frequency stability is among the major concerns for the system operators as the inertia levels are dramatically reducing [2]. In addition, as the penetration levels of renewable energy sources and electric vehicles are expected to rise in low-voltage distribution grids, the system will be more vulnerable during voltage and frequency disturbances. Thus, the capabilities of power electronic converters and the flexibilities offered by energy storage systems need to be exploited to secure the proper operation of the distribution grid by designing tailor-made support strategies for storage systems.

Smart inverters can offer flexible capabilities to the system operators under normal and abnormal conditions. There are already commercial inverters that can provide voltage and frequency support during disturbances by controlling the reactive and active power respectively [3]. Further, synthetic inertia provision by wind turbines has successfully been demonstrated by Hydro-Quebec and

widespread adoption is expected [4]. More advanced schemes have also been proposed considering balanced and unbalanced conditions [5]-[7]. The implementation of these schemes requires the development of more advanced current controllers which are capable of regulating both positive and negative sequence currents [8]-[10]. In addition, a voltage and frequency support strategy is proposed for a storage system in [11]. However, the authors did not consider fair compensation between the two services, which cannot secure the provision of concurrent frequency and voltage support. To secure proper operation under any grid conditions, the authors in [12] developed a scheme for a fair compensation of voltage and frequency provision. Therefore, the new operating modes can be utilized to improve the stability of the distribution grid.

The unique characteristics of the distribution network are not considered by the studies mentioned above. The resistive nature of the distribution lines alongside with the capabilities of power converters should be taken into account in order to develop dedicated control strategies for the low voltage distribution grid. More specifically, the decoupled control approach is not valid in distribution networks due to the low inductance to resistance ratio of the grid impedance. Consequently, voltage support should be provided not only with reactive current, but also with active current to ensure effective operation. A current reference generator that is based on the grid impedance for balanced and unbalanced conditions is proposed in [13]; however no formulation for voltage support is considered. Further, an optimization algorithm is developed to maximize the voltage support and unbalance compensation in distribution networks [14]. The objective function tries to maximize the difference between positive and negative sequence voltage to compensate both voltage drops and unbalances. Nevertheless, the authors in [14] assume that the converter should support the voltage with its rated current regardless of the voltage drop intensity. This approach can be considered to be simple in terms of implementation complexity, but the large discontinuities in the voltage support concept can impose intense oscillations. In this paper the conventional voltage support of [12] is modified to provide proper support to the distribution network where simultaneous injection of active and reactive power is essential for supporting the voltage. In addition, a droop control is implemented to adjust the output current according to the voltage drop intensity which is not considered in [14]. Further, a second modification is applied for concurrent operation of voltage and frequency provision where the support is prioritized according to the severity of the event. Therefore, a new voltage and frequency support scheme is proposed in this paper dedicated for storage systems connected in low-voltage distribution grids. The effectiveness of the support scheme is tested on a Flywheel Energy Storage System (FESS). It should be noted that the same support strategy can be applied in a battery storage system as well.

Section 2 of the paper describes the existing voltage and frequency support methodologies. The proposed support strategy is presented in Section 3 and the simulation results of a FESS enhanced with the proposed voltage-frequency support strategy is presented in Section 4. The proposed strategy is validated in a prototype experimental setup as demonstrated in Section 5. Finally, Section 6 concludes the paper.

2. Conventional Voltage-Frequency Support Schemes

Voltage should lie within safe limits to secure proper operation and avoid voltage collapse with severe consequences. The distribution grid faces radical changes that can increase the sources of voltage disturbances. More specifically, in contemporary distribution grids the short-circuit faults and the connection of heavy loads is usually the main reasons for voltage drops. In the future distribution network, the sources of voltage drops is expected to increase due to the integration of electrical vehicles into the distribution grid that require a significant power demand for charging. In addition, renewable generation can cause reverse power flow leading to over-voltage conditions. Hence, securing voltage stability is becoming more challenging than ever for the system operators. According to the grid codes, renewable energy sources should remain connected with the grid and provide Fault Ride Through (FRT) operation during disturbances. The provision of voltage support is realized by the injection of reactive current (i_Q) which is defined as the current that lags the voltage by 90 degrees. The reactive current is altered as in (1) according to the voltage drop intensity,

$$i_Q = k_v (V_n - V_{PCC}) = k_v \Delta V \quad (1)$$

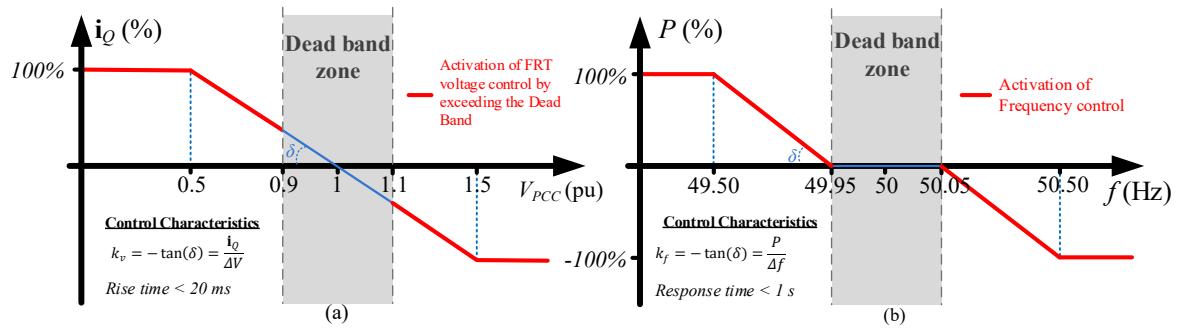


Fig. 1: Conventional voltage and frequency support schemes: (a) Voltage support and (b) frequency support.

where, V_n and V_{PCC} are the magnitude of the nominal voltage and of the voltage at the Point of Common Coupling (PCC) respectively. The voltage droop constant (k_v) determines the voltage support intensity and should be equal to or higher than 2 according to the grid codes [12]. The provision of voltage support is enabled when the voltage exceeds a pre-defined dead-band zone as shown in Fig. 1(a). Further, the converter current ratings during the voltage support should be considered to avoid overcurrent protection tripping and excessive thermal loading. Hence, the active current (i_P), which is defined as the current vector that is in-line with the voltage vector and is responsible for the active power injection, should be limited according to the rated current (I_n) of the inverter, as given in (2).

$$i_P = \sqrt{I_n^2 - i_Q^2} \quad (2)$$

Frequency stability is also deteriorated due to the decrease of the physical inertia of the system caused by the high penetration of power electronics based distributed resources. The number of frequency incidents have increased over the last years due to lack of active power control for frequency regulation [2]. Hence, load shedding and renewable generation curtailment is implemented to deal with under- and over-frequency disturbances respectively. In addition, de-loading operation of renewable generation is proposed to enable them to respond in under and over-frequency events. Fig. 1(b) shows a frequency support strategy especially designed for storage systems (enhanced frequency response) in the UK [15]. The active power (P) is regulated according to the frequency variations and the frequency droop constant (k_f) which defines the intensity of the frequency support as in,

$$P = k_f (f_n - f) = k_f \Delta f \quad (3)$$

where, f_n is the nominal frequency. It should be highlighted that when a grid fault occurs, it usually affects both voltage and frequency [12]. For instance, a high value of voltage droop constant will deteriorate the frequency support capability and vice versa. Therefore, a fair compensation of voltage and frequency support is essential to secure proper grid support under high penetration scenarios of renewable generation in the distribution grid.

3. Proposed Voltage-Frequency Support Scheme

The conventional support strategies (as mentioned in Section 1) are not effective in distribution networks due to the resistive characteristic of the distribution lines. The control of reactive current to provide voltage support assumes that the grid impedance is mainly inductive or the X/R ratio is high. However, this assumption for decoupled control is only valid in transmission networks. Therefore, the grid resistance and inductance should be both considered when designing voltage support strategies for distribution networks.

A distributed generator (i.e., PV, wind, storage, etc.) connected to the grid through the PCC can be seen as a simple Thevenin circuit which is constituted by a grid impedance ($Z=R+jX$) and a main grid voltage (v_g). Therefore, the voltage at the PCC can be expressed as,

$$\mathbf{v}_{PCC} = \mathbf{v}_g + \mathbf{i}R + \mathbf{i}X \quad (4)$$

where $\mathbf{v}_g = [v_{gd} \ v_{gq}]^T$ is the grid voltage vector, $\mathbf{v}_{PCC} = [v_{PCCd} \ v_{PCCq}]^T$ is the PCC voltage vector, $\mathbf{i} = [i_d \ i_q]^T$ is the current vector (all expressed in the synchronous reference dq -frame), R is the grid resistance and X is the grid reactance. At the transmission level, the term $\mathbf{i}R$ is neglected since it is very small compared to the term $\mathbf{i}X$ and the voltage support is achieved when only reactive current is injected. However, in the case of distribution networks, the X/R ratio is considerably lower and both terms ($\mathbf{i}R$ and $\mathbf{i}X$) need to be included in the voltage support strategy. Therefore, the current should consist of active (\mathbf{i}_{PFRt}) and reactive (\mathbf{i}_{QFRt}) current as,

$$\mathbf{i} = \mathbf{i}_{PFRt} + j \cdot \mathbf{i}_{QFRt} = I_{FRT} \angle \theta_{opt} \quad (5)$$

where I_{FRT} the current magnitude during the voltage support and $\theta_{opt} = \tan^{-1}(X/R)$ is the phase angle of the support current vector. It should be highlighted that θ_{opt} is the current phase angle that ensures the optimal voltage support according to the X/R characteristics of the distribution line.

The proposed voltage support strategy is illustrated in Fig. 2(a). According to the proposed scheme, the FRT operation is enabled when the voltage exceeds the dead-band zone defined as $0.9 \leq V_{PCC} \leq 1.1$ pu. Then, a droop control approach is utilized to adjust the current magnitude according to the intensity of the voltage drop. The voltage droop constant (k_v) is defined in an adaptive way considering both voltage drop and operating conditions before the event, as given in,

$$k_v = \frac{I_{FRT} - I_0}{\Delta V(I_n - I_0)} \quad (6)$$

where I_0 is the operation current before the voltage drop. The proposed voltage support scheme is tailored for storage devices, which can both absorb and inject energy. However, the scheme can be applied in any renewable generation unit with slight modifications. As can be seen from Fig. 2(b), the current angle is equal to θ_{opt} during under-voltage conditions (discharging mode) and equal to its supplementary ($180 - \theta_{opt}$) during over-voltage conditions (charging mode).

The conventional frequency support (as shown in Section 1) can also be represented in terms of current magnitude (I) and current angle (θ) as shown in Fig. 2(c) and 2(d). As can be seen, the current magnitude is altered with respect to the frequency drop intensity as in,

$$k_f = \frac{I_f - I_0}{\Delta f(I_n - I_0)} \quad (7)$$

where I_f is the frequency support current and k_f the frequency droop constant. For under-frequency events, the angle is maintained at zero degrees since only active power is injected into the grid

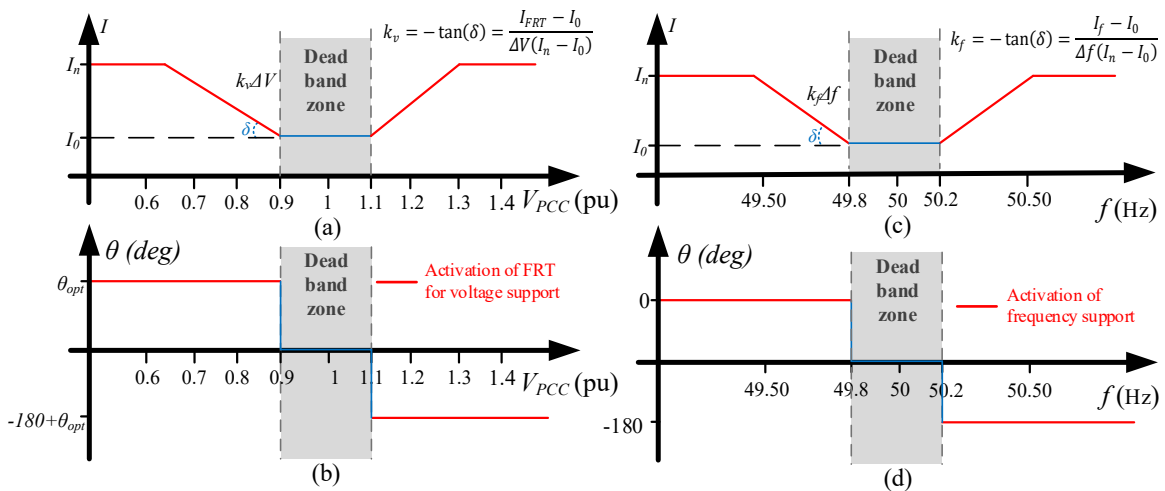


Fig. 2: Proposed voltage and frequency support strategies: (a) Current magnitude for voltage support, (b) current angle for voltage support, (c) current magnitude for frequency support and (d) current angle for frequency support.

(discharging mode), while in case of over-frequency, active power should be absorbed by the storage system. Hence the angle should be maintained at -180 degrees (charging mode). It should be highlighted that the representation of the frequency support using the current magnitude and angle is adopted in order to develop the proposed voltage-frequency support scheme, as demonstrated in the following paragraphs.

A mixture of voltage and frequency provision is developed by combining the schemes described above. The proposed strategy ensures a proper and fair compensation between voltage and frequency under any grid conditions. The current magnitude during voltage and/or frequency support (I_{V-f}) according to the proposed methodology is defined as,

$$I_{V-f} = I_0 + (k_v k_1 \Delta V + k_f k_2 \Delta f)(I_n - I_0) \quad (8)$$

where k_1 and k_2 are the parameters that ensure a fair compensation between voltage and frequency support and are defined as,

$$k_1 = \frac{\Delta V}{\Delta V + \Delta f}, \quad k_2 = \frac{\Delta f}{\Delta V + \Delta f} \quad (9)$$

It should be noted that the values of k_1 and k_2 can only be in the range $[0, 1]$. As can be seen, k_1 and k_2 are complementary terms and their sum should always be equal to one. In addition, it should be highlighted that k_1 and k_2 are defined only in case of voltage and/or frequency violation (outside of dead-band zone or zones).

According to the proposed strategy, the current angle is expressed in degrees ($^\circ$) and it is given by,

$$\theta_{V-f} = \begin{cases} k_1 \cdot \theta_{opt} + k_2 \cdot 0^\circ & V \downarrow, f \downarrow \\ k_1 \cdot \theta_{opt} - k_2 \cdot 180^\circ & V \downarrow, f \uparrow \\ k_1 \cdot (\theta_{opt} - 180) - k_2 \cdot 180^\circ & V \uparrow, f \uparrow \\ k_1 \cdot (\theta_{opt} - 180) + k_2 \cdot 0^\circ & V \uparrow, f \downarrow \end{cases} \quad (10)$$

There are four possible angle equations according to the event type as shown in (10):

- Under-voltage ($V \downarrow$) and under-frequency ($f \downarrow$) where θ_{V-f} can be calculated between 0° (full active power injection during under-frequency event only) and θ_{opt} (during under-voltage event only)
- Under-voltage ($V \downarrow$) and over-frequency ($f \uparrow$) where θ_{V-f} can vary between θ_{opt} (during under-voltage event only) and -180° (charging during over-frequency event only)
- Over-voltage ($V \uparrow$) and over-frequency ($f \uparrow$) where θ_{V-f} can vary between -180° (absorbing active power during over-frequency event only) and $\theta_{opt} - 180$ (during over-voltage event only) which is the supplementary angle of θ_{opt}
- Over-voltage ($V \uparrow$) and under-frequency ($f \downarrow$) where θ_{V-f} can be calculated between 0° (injection of active power during over-frequency event only) and $\theta_{opt} - 180$ (during over-voltage event only)

Since the current magnitude and angle are defined, the current vector during the proposed support (\mathbf{i}_{V-f}) can be defined as,

$$\mathbf{i}_{V-f} = I_{V-f} \angle \theta_{V-f} = [\mathbf{i}_{P-V-f} \quad \mathbf{i}_{Q-V-f}]^T \quad (11)$$

4. Simulation Results

The proposed strategy is implemented on a 1 kW/2 kWh flywheel energy storage system with rated speed 14000 rpm modelled in MATLAB/Simulink to investigate the additional capabilities of storage devices operating with the proposed FRT scheme. It should be highlighted that the proposed voltage-frequency support scheme can also be applied to any type of storage systems (e.g., chemical batteries). A detailed model of the flywheel and its associated controllers is illustrated in Fig. 3. The model consists of a permanent magnet generator, whose inertia also includes the flywheel mass inertia, and a back-to-back converter configuration along with its controller. The machine side converter (MSC) controls the generator speed or active power, while the grid side converter (GSC) regulates the dc-link voltage and

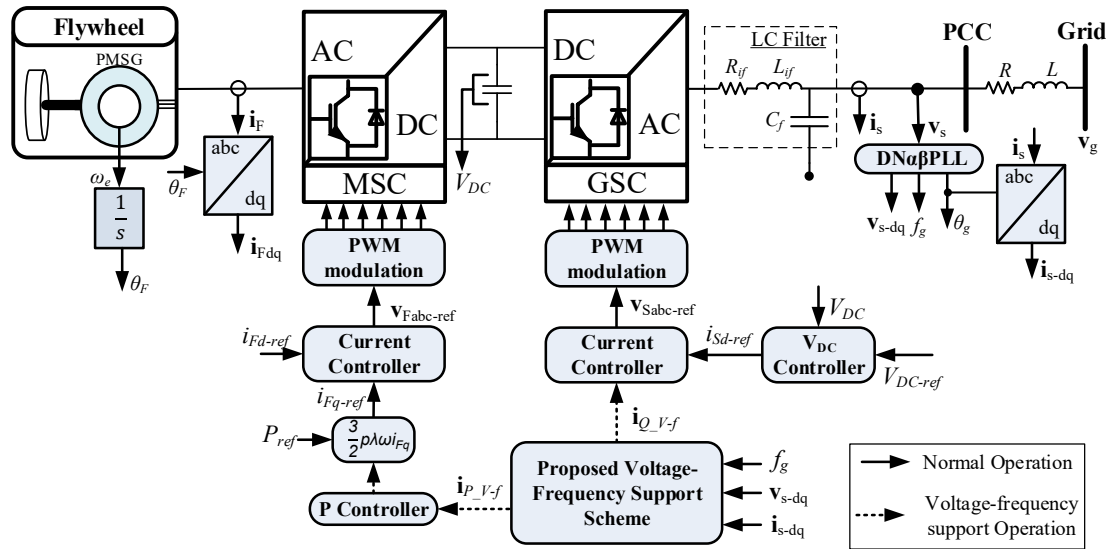


Fig. 3: FESS enhanced with the proposed voltage and frequency support scheme.

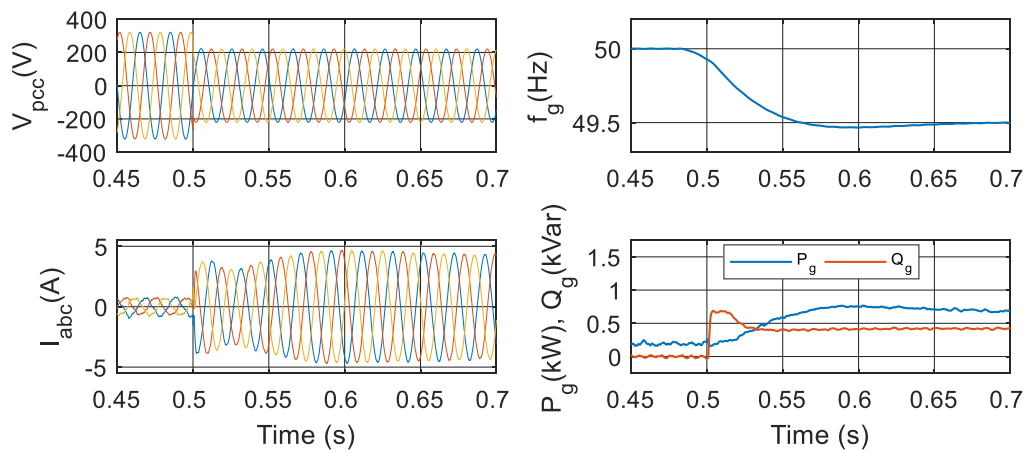


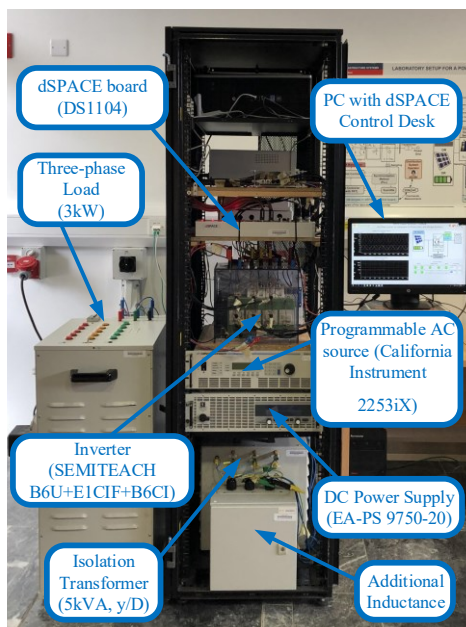
Fig. 4: Simulation results for instantaneous voltage-frequency drop.

reactive power. The MSC controller is implemented using vector control as in [16]. More specifically, the d -axis is aligned with the rotor flux and the q -axis is 90 degrees behind the d -axis to enable a decoupling control technique. Hence, only the q -axis contributes to torque production and the d -axis reference current is always set to zero. Further, the tuning of the PI current controllers and the DC-link controller is implemented as in [17]. The reactance to resistance (X/R) ratio is assumed to be 2.3658 which is a typical value for low voltage distribution grids.

The performance of the proposed voltage-frequency support strategy is firstly validated through simulations. A balanced three-phase fault is applied to the grid at $t=0.5$ s which causes a voltage drop of 30% at the PCC as shown in Fig. 4. Further, the scenario considers that the voltage drop also causes the tripping of a generator in the grid and thus, an under-frequency event of 0.5 Hz ($\Delta f=100\%$) occurs at $t=0.5$ s. As can be seen, initially, the reactive power increase due to the faster dynamics of the voltage drop event compared to the slower dynamics of the frequency change event. Then, a few milliseconds later, the frequency exceeds its dead-band zone as defined in Fig. 2 and the frequency support is activated as well, which cause the decrease of the reactive power and the increase of the active power. It is important to note that in this case, frequency support is more intense compared to voltage support since the frequency deviation is greater than the voltage deviation.

5. Experimental Results

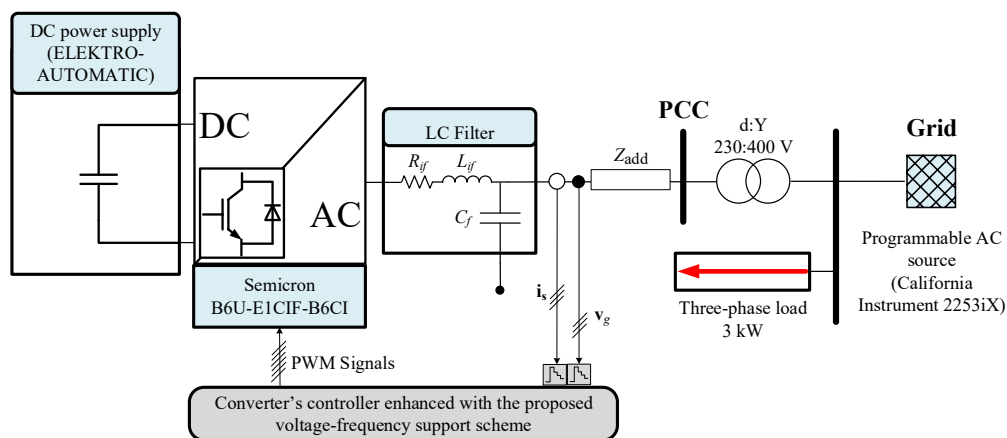
An experimental setup has been developed to validate the performance of the proposed voltage-frequency support scheme. A three-phase 5 kVA SEMIKRON Semiteach (B6U+E1C1F+B6CI) has been used as GSC and the GSC control has been developed with a dSPACE DS-1104 DSP board with sampling and switching frequency of 3.45 kHz. A DC power supply (ELEKTRO-AUTOMATIC) has been utilized to emulate the flywheel along with the MSC or a chemical battery storage unit. The inverter has been connected through an LC filter and an inductance into a programmable AC source (California Instrument 2253iX) which has been used to play the role of the grid. In addition, a 3 kVA three-phase load has been connected in parallel with the AC source (since the AC source can only support two-quadrant operation for only delivering power). Further, a 5 kVA Y/D transformer has been utilised to ensure grid isolation. The current rating of the three-phase converter is 10 A, however, due to the limited capacity of the three-phase load the converter current was limited to 3.88 A rms to ensure that the AC source will never absorb energy. The parameters of the experimental are depicted in Table I. The grid impedance used for the simulation results is also utilised for the experimental setup. Fig. 5 demonstrates a photo



(a)

Table I: Parameters of the experimental setup

Switching and sampling frequency	3.45 kHz
Synchronization Unit	DN α β -PLL ($k_p=92$, $T_i=0.000235$)
Current Controller	$k_p=17.3$, $k_f=218.5$
LC Filter	$R_{if}=0.19 \Omega$, $L_{if}=15$ mH, $C_{if}=9.45 \mu\text{F}$
Additional Inductance	$Z_{add} = 4.7$ mH



(b)

Fig. 5: (a) A photo of the laboratory setup, (b) Schematic diagram of the setup.

and the schematic diagram of the laboratory setup that has been developed to validate the proposed support strategy.

Three sets of experiments have been conducted to investigate the effectiveness of the voltage-frequency support scheme. The first case study investigates the performance of the proposed scheme under a voltage sag. The programmable AC source has been used to create the voltage sag by adjusting its voltage from 230 V to 161 V which represents a 30% reduction. Fig. 6 demonstrates the transient response of the experimental setup when the proposed support strategy is activated by the voltage sag. Prior the voltage drop, the inverter was producing 550 W as shown in Fig 6(c). However, when the voltage support scheme was enabled, the current of the inverter increased as demonstrated in Fig. 6(b) to support the grid during the under-voltage event. It should be noted that the current provided during

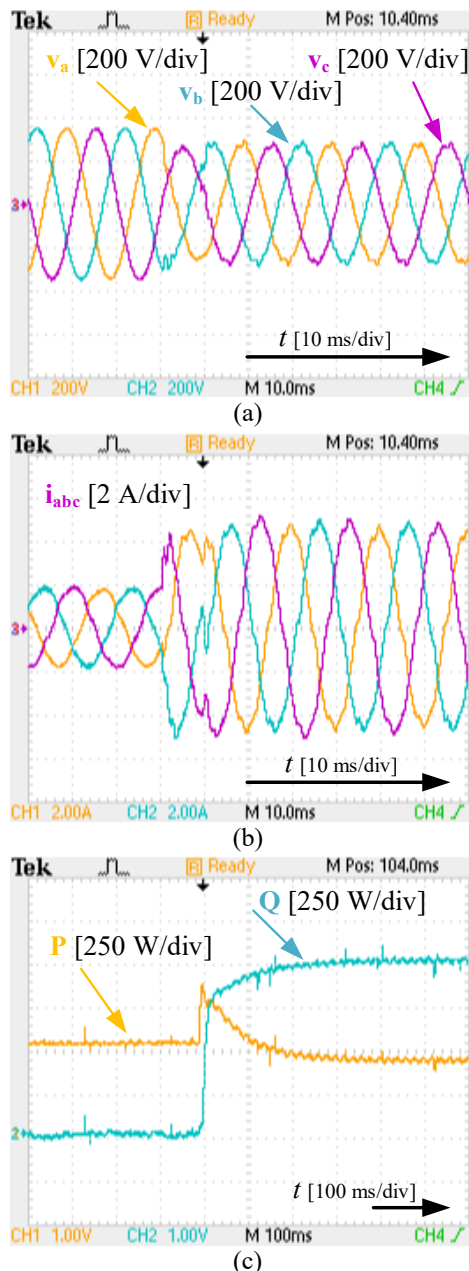


Fig. 6: Experimental results for under-voltage event with the proposed support strategy (a) Grid voltage, (b) output current of storage, (c) active and reactive power of storage unit.

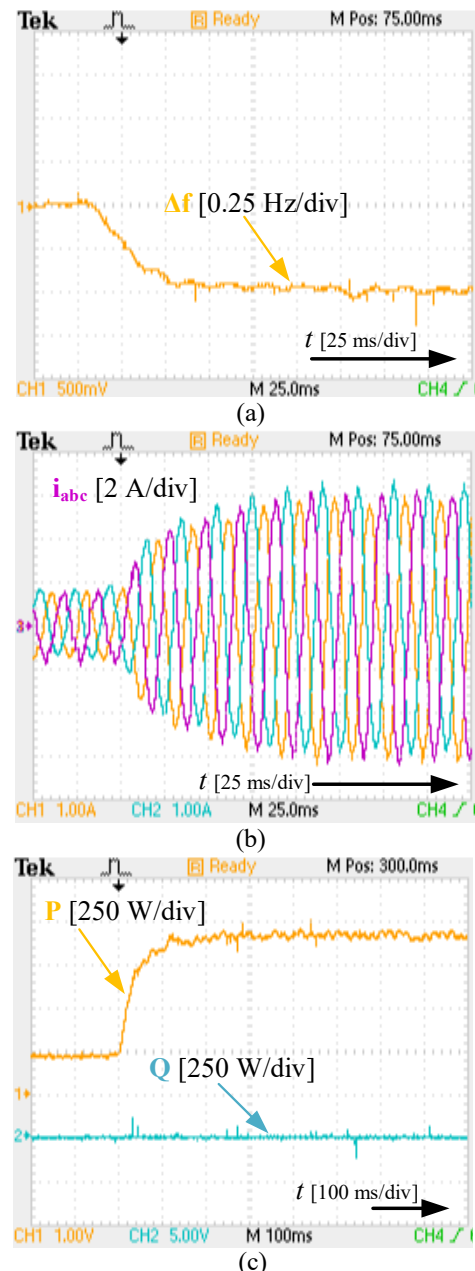


Fig. 7: Experimental results for under-frequency event with the proposed support strategy (a) Grid voltage, (b) output current of storage, (c) active and reactive power of storage unit.

the voltage support is limited to the inverter rating in order to avoid overloading conditions. According to the proposed FRT scheme, during the voltage sag, the power injection of the inverter is changed to provide $Q=1010$ VAR and $P=450$ W which is in line with the optimal voltage support (as proposed in Fig. 2) considering the X/R ratio of the distribution line.

The second case study examines the performance of the proposed scheme during under-frequency events. A frequency drop of 0.5 Hz is emulated through the AC source as shown in Fig 7(a). Initially, the storage unit was producing 200 W. The activation of the frequency support mode imposes additional active power to be produced according to (8) and (10) while the reactive power injection remains unaffected as shown in Fig. 7(c). This is also validated in Fig. 7(b), where the current increases until reaching their rating value during the under-frequency event in order to support the frequency stability of the grid. The last case study can be considered as a mixture of the first two studies. Both under-frequency and under-voltage events are generated simultaneously through the programmable AC source as shown in Fig. 8(a) and Fig. 8(b). A voltage step change from 230 V to 161 V is generated and at the same time a frequency step change of 0.5 Hz is also created. The storage unit is producing 200 W prior the activation of the voltage-frequency support as shown in Fig. 8(d). The activation of the voltage support mode is enabled first due to the faster dynamics of the voltage sag. Hence, initially the reactive power is increased to support the grid voltage as demonstrated in Fig. 8(d). Then, the under-frequency detection signal is enabled few a milliseconds later due to the slower dynamics of the frequency and both active and reactive power are adjusted to 810 W and 340 Var respectively to support both events. The frequency support is more intense in this case since the frequency drop is more severe due to higher deviation of the frequency from the nominal value than the voltage deviation. The proposed support scheme illustrates that the storage inverter can share the support of frequency and voltage and provide a more appropriate support to the distribution grid considering the disturbance characteristics and the distribution line characteristics. Therefore, the capability of storage systems to provide both voltage and frequency support instantaneously have been demonstrated through experimental tests.

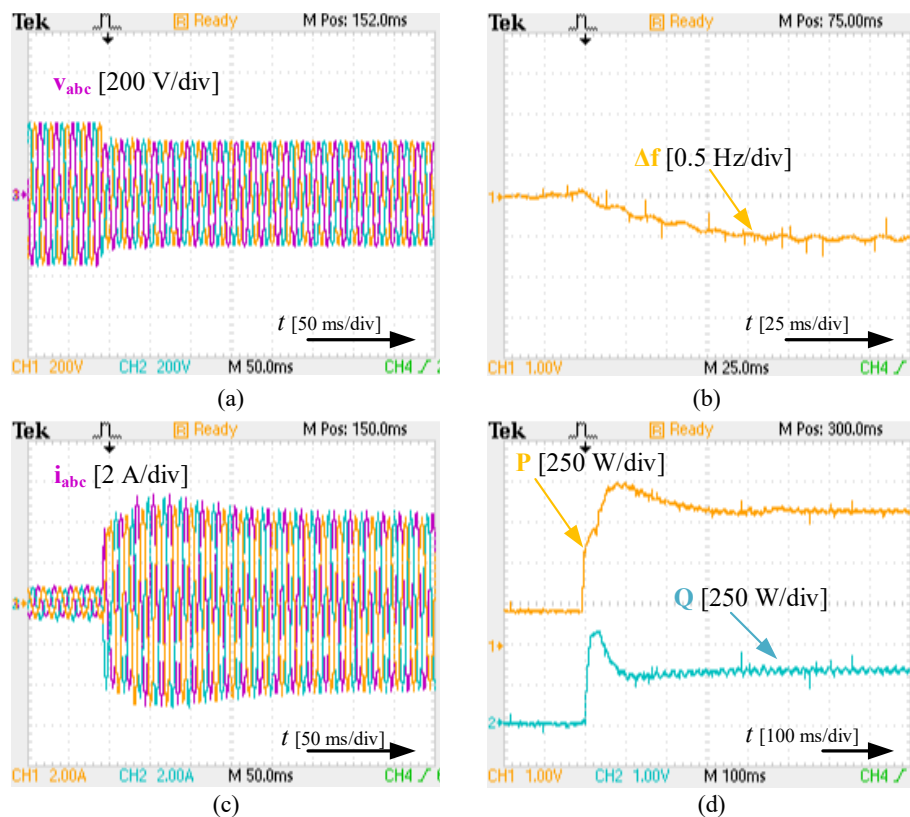


Fig. 8: Experimental results for both under-voltage and under-frequency events with the proposed support strategy. (a) Grid voltage, (b) grid frequency deviation, (c) output current of storage (d) active and reactive power of storage unit.

Conclusion

The proposed support scheme enables the fair compensation between voltage and frequency provision for storage systems connected to distribution grids. The proposed solution utilizes the knowledge of the grid impedance for the development of a tailor-made solution for distribution grids. The support scheme is applied to a FESS, however it can be used in any type of storage systems. Simulation and experimental tests were carried out to validate the performance of the proposed voltage-frequency support scheme. The proposed strategy shows that a power electronics based energy storage system can dynamically support the grid voltage and frequency and it is capable to adjust its support based on the severity of voltage or frequency deviations. The results indicate that storage units can support voltage and frequency events at the same time, which can have a great impact on the stability of the distribution grid.

References

- [1] Y. Yang, P. Enjeti, F. Blaabjerg and H. Wang, "Wide-scale adoption of photovoltaic energy: Grid code modifications are explored in the distribution grid," *IEEE Ind. Applications Magazine*, vol. 21, no. 5, pp. 21-31, Sep.-Oct. 2015.
- [2] J. Fang, H. Li, Y. Tang and F. Blaabjerg, "On the inertia of future more-electronics power systems," *IEEE Journal Emerg. Sel. Topics Power Electron.*, pp. 1-19, Oct. 2018 (in press).
- [3] PV grid integration, SMA Solar Technology. Niestetal, Germany, 2012. [Online]. Available: <https://www.sma.de/en>.
- [4] Technical requirements for the connection of generation facilities to the Hydro-Quebec transmission system, Hydro-Quebec. Montreal, Canada, 2003. [Online]. Available: <http://www.hydroquebec.com>.
- [5] A. Camacho, M. Castilla, J. Miret, R. Guzman, and A. Borrell, "Reactive power control for distributed generation power plants to comply with voltage limits during grid faults," *IEEE Trans. Power Electron.*, vol. 29, no. 11, pp. 6224-6234, Nov. 2014.
- [6] P. Rodriguez, A. V. Timbus, R. Teodorescu, M. Liserre, and F. Blaabjerg, "Flexible active power control of distributed power generation systems during grid faults," *IEEE Trans. Ind. Electron.*, vol. 54, no. 5, pp. 2583-2592, Oct. 2007.
- [7] A. Camacho, M. Castilla, J. Miret, J. C. Vasquez, and E. Alarcon-Gallo, "Flexible voltage support control for three-phase distributed generation inverters under grid fault," *IEEE Trans. Ind. Electron.*, vol. 60, no. 4, pp. 1429-1441, Apr. 2013.
- [8] L. Hadjidemetriou, E. Kyriakides and F. Blaabjerg, "A robust synchronization to enhance the power quality of renewable energy systems," *IEEE Trans. Ind. Electron.*, vol. 62, no. 8, pp. 4858-4868, Aug. 2015.
- [9] Z. Ali, N. Christofides, L. Hadjidemetriou, and E. Kyriakides, "An advanced current controller with reduced complexity and improved performance under abnormal grid conditions," in *Proc. IEEE Manchester PowerTech*, 2017, pp. 1-6.
- [10] L. Hadjidemetriou and E. Kyriakides, "Accurate and efficient modelling of grid tied inverters for investigating their interaction with the power grid," in *Proc. IEEE Manchester PowerTech*, 2017, pp. 1-6.
- [11] E. Serban, M. Ordonez and C. Pondiche, "Voltage and frequency grid support strategies beyond standards," *IEEE Trans. Power Electron.*, vol. 32, no. 1, pp. 298-309, Jan. 2017.
- [12] L. Hadjidemetriou, P. Demetriou and E. Kyriakides, "Investigation of different fault ride through strategies for renewable energy sources," in *Proc. IEEE Eindhoven PowerTech*, 2015, pp. 1-6.
- [13] A. Camacho, M. Castilla, J. Miret, L. G. de Vicuña and R. Guzman, "Positive and negative sequence control strategies to maximize the voltage support in resistive-inductive grids during grid faults," *IEEE Trans. Power Electron.*, vol. 33, no. 6, pp. 5362-5373, June 2018.
- [14] X. Guo, W. Liu, X. Zhang, X. Sun, Z. Lu and J. M. Guerrero, "Flexible control strategy for grid-connected inverter under unbalanced grid faults without PLL," *IEEE Trans. Power Electron.*, vol. 30, no. 4, pp. 1773-1778, Apr. 2015.
- [15] K. Smethurst, S. Williams, and V. Walsh, "Testing guidance for providers of enhanced frequency response balance service," National Grid, UK, Mar. 2017.
- [16] R. Xiang, X. Wang and J. Tan, "Operation control of flywheel energy storage system with wind farm," in *Proc. of the 30th Chinese Control Conference*, Yantai, 2011, pp. 6208-6212.
- [17] C. Bajracharya,, M. Molinas, J. A. Suul, and T. M. Undeland, "Understanding of tuning techniques of converter controllers for VSC-HVDC," presented at the Nordic Workshop Power Ind. Electron., Espoo, Finland, 2008.